of processes that occur during a single encounter should be considered parts of a concerted event even though the members of the set do not necessarily begin and end simultaneously.

Above 1 ML, bromoethane is clearly preferred. We now estimate a lower limit for the percentage of consumed DBr which enters this channel. Assuming that the extent of DBr dissociation is the same with and without ethylene, we compute the following percentages: 75%, 12.5%, and 12.5% for bromoethane formation, ethane formation, and DBr dissociation, respectively. The product, bromoethane, is itself photoactive,[3] but its concentration is not high enough here to compete with the reaction between deuterium bromide and ethylene.

It is interesting that the photoreactivity depends on the structure of ethylene. At the same surface concentration, π-bonded ethylene produces $\approx$10 times more ethane and bromoethane than di-σ-bonded ethylene. These differences emphasize the role played by the substrate; different adsorption sites involve different adsorbate substrate bonding. In turn, intraadsorbate electronic structures differ. Both can play important roles indicating surface photoreactivity.

4. Summary

1. DBr adsorbed on Pt(111) partially decomposes at 52 K. Irradiation with UV light from a Hg arc lamp causes further dissociation, a substrate-mediated process attributed to excitation by attachment to DBr of subvacuum hot electrons. Only the first layer of multilayer DBr is photoactive.

2. There is no thermal reaction between coadsorbed C_2H_4 and DBr. Ethylene alone is not photolyzed; i.e., no photoinduced desorption, decomposition or transformation among its adsorption states occur. There is no photoassisted hydrogenation reaction between ethylene and chemisorbed hydrogen.

3. Coadsorbed DBr and C_2H_4 are photoactive, producing adsorbed ethane and bromoethane which desorb subsequent TPD.

4. The photoinduced ethane formation is attributed to the photodissociation of DBr, generating energetic D atoms. These react with coadsorbed ethylene to produce surface-bound ethyl species, which react thermally with DBr, probably during TPD, to form ethane.

5. The proposed pathway to bromoethane involves a concerted reaction involving surface-aligned and oriented reactant pairs, i.e., DBr–C_2H_4. The excitation is provided by electrons, excited in the substrate, which attach to DBr.

6. The photoproducts form with higher probability when ethylene is π-bonded rather than di-σ-bonded.

Acknowledgment. This work was supported in part by the National Science Foundation, Grant CHE 9015600.

The Electronic Nature of the Metal–Metal Quadruple Bond: Variable Photon Energy Photoelectron Spectroscopy of $Mo_2(O_2CCH_3)_4$

Dennis L. Lichtenberger,*,† Charles D. Ray,† Frank Stepniak,‡ Yu Chen,‡ and J. H. Weaver‡

Contribution from the Laboratory for Electron Spectroscopy and Surface Analysis, Department of Chemistry, University of Arizona, Tucson, Arizona 87521, and Department of Chemical Engineering and Materials Science, University of Minnesota, Minneapolis, Minnesota 55455.
Received July 24, 1992

Abstract: Variable-energy photoelectron spectroscopy of thin film $Mo_2(O_2CCH_3)_4$ on a GaAs substrate in ultrahigh vacuum is used to examine the valence ionizations of the quadruple metal–metal bond. The changes in photoionization cross sections with photon energy over a range of 40 to 90 eV are examined. The metal-based σ, π, and δ ionizations of the quadruple bond are strongly enhanced relative to the acetate-based ionizations in the region of photon energies from 40 to 50 eV. This is consistent with a molybdenum 4p to 4d resonance and super-Coster–Kronig Auger enhancement of the metal-based ionizations. The extent of resonance enhancement is related to the amount of Mo 4d character associated with the ionization. The π ionization of the Mo–Mo quadruple bond has the largest contribution from the Mo 4d orbitals. The δ and σ ionizations of the metal–metal bond contain smaller amounts of Mo 4d character, and some Mo 4d character is observed in the acetate-based ionizations. This is explained in terms of significant overlap and mixing of the δ and σ components with the ligand orbitals. Also, in the case of the σ component, there is a possible filled/filled interaction between the Mo $4d_{z^2}$ orbital on one metal and the Mo $4p_z$ orbital on the adjoining metal. These interactions have significant impact on the properties of these complexes.

Introduction

Following the recognition that certain molybdenum dimer complexes possess metal–metal quadruple bonds,[1] there has been a continuing effort directed toward obtaining a better understanding of these compounds.[2-4] Recent investigations range from studies of general reactivity[5] to studies of these compounds as precursors for cluster formation[6] and as monomeric units in inorganic polymerization reactions.[7] There have even been several industrially useful catalysts identified which contain Mo–Mo quadruple bonds.[8] In each of the studies, the focus of the effort

* Author to whom correspondence should be addressed.
† University of Arizona.
‡ University of Minnesota.

(1) (a) Lawton, D.; Nason, R. *J. Am. Chem. Soc.* **1965**, *31*, 921 for report of compound. (b) Cotton, F. A. *Inorg. Chem.* **1965**, *4*, 334. (c) Cotton, F. A.; Durkis, N. F.; Harris, C. B.; Johnson, B. F. G.; Lippard, J.; Mague, J. T.; Robinson, W. R.; Wood, J. S. *Science* **1964**, *145*, 1305 for construct of metal–metal bond.

(2) Lichtenberger, D. L.; Johnson, R. L. *Metal–Metal Bonds and Clusters in Chemistry and Catalysis*; Fackler, J. P., Jr., Ed.; Plenum: New York, 1989, and references therein.

(3) Blevins, C. H. *Diss. Abstr. Int.* **1984**, *B45*, 1186.

(4) Trogler, W. C.; Gray, H. B. *Acc. Chem. Res.* **1978**, *11*(6), 232 and references therein.

0002-7863/92/1514-10492$03.00/0

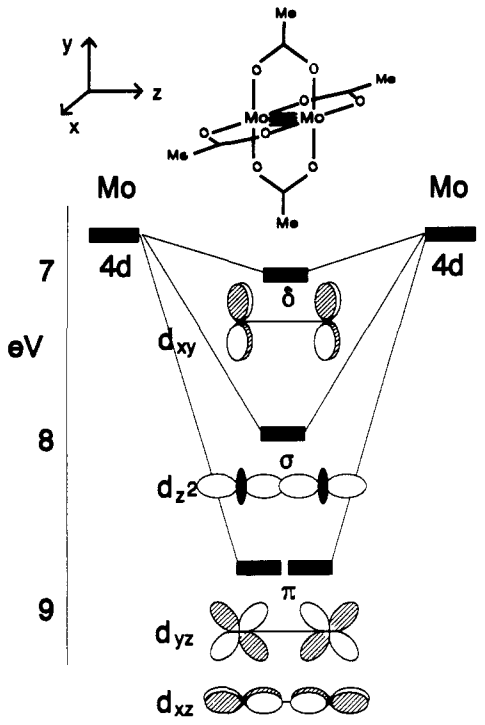

Figure 1. Orbital construct of the metal–metal bond in $Mo_2(O_2CCH_3)_4$. The δ and π levels are placed at their gas-phase values. The σ level is placed according to observations in the surface experiments.

has been on the structure and reactivity of the metal–metal bond. Several aspects of the electronic structure of the metal–metal quadruple bond in these complexes are only partly understood. Key questions concern the strength and nature of the δ bond, and the surprising characteristics of the σ bond.[2] Much of the attention has now turned to questions of the mutual electronic interactions between the quadruple bonds and the ligand environment. Additional information is needed to allow a better understanding of the properties of these complexes. This is the focus of the present photoelectron study of $Mo_2(O_2CCH_3)_4$ using synchrotron radiation.

Because of their ease of preparation, stability, and volatility, the tetracarboxylate compounds of dimolybdenum, especially $Mo_2(O_2CCH_3)_4$, have been the subject of most experimental studies of the $[M^4\text{–}M]^{4+}$ moiety.[3,4,9-11] Ultraviolet photoelectron spectroscopy (UPS) has proven to be a powerful tool in probing the electronic structure of these compounds.[2,3,10-13] The emphasis of these efforts has been to investigate the nature of the σ, π, and δ components of the metal–metal bonding interactions. These UPS studies have resulted in the assignment of the ionization energies of the metal–metal bond.[2,12] A simple construct of the metal–metal symmetry interactions with ionization energies from the UPS studies relative to the vacuum level is shown in Figure 1.[2,12] In addition to the general assignment of the ionizations, some interesting features of this M–M quadruple bond have been indicated by these studies. For instance, we have observed vibrational fine structure in the δ ionization,[11] and this information coupled with other properties of related molecules led us to the proposal of significant oxygen character from the ligands contributing to the δ symmetry interaction.[2] A more substantial contribution to the Mo–Mo bond is provided by the π symmetry interaction, and the ionization corresponding to this π orbital leads to a broad vibrational progression.[2] One of the most difficult challenges has been the assignment and interpretation of the Mo–Mo σ bond ionization. The present interpretation is that the σ ionization is nearly coincident with the π ionization and has little net metal–metal bonding character. The experimental support for these characteristics is quite limited at present, and additional evidence is needed to support this understanding of the $[M^4\text{–}M]^{4+}$ moiety.

Several recent studies by Green[14-17] and Solomon[18-20] have shown the utility of variable photon energy photoelectron spectroscopy in probing the electronic structure of discrete transition metal complexes. The focus of these studies has been on examination of valence ionizations as a function of the energy of incident photons using synchrotron radiation. Every atomic orbital ionization has its own characteristic cross-section dependence on photon energy, and in appropriate conditions resonance effects may also enhance the ionization. The cross section for ionization from each orbital of every atom has been calculated[21] for a large range of incident photon energies. The ionizations of molecules show similar effects, which are largely traced to the atomic orbital contributions. Deviations from the atomic contributions can occur with low photon energies or with rearrangements in the final state, but neither is expected to be of major importance in the present case. Hence, knowledge of the change in cross section of a specific ionization band with excitation energy allows one, in principle, to determine the amount of metal or ligand character associated with that particular ionization. The studies of Green and Solomon have demonstrated the information that can be provided from this approach for transition metal complexes, and set the foundation for the present investigation.

We report here the first variable photon energy photoelectron experiment on a metal–metal multiple-bonded species. The complex chosen for study is $Mo_2(O_2CCH_3)_4$. These experiments complement previous photoelectron and computational studies by providing additional evidence of the character of the σ, π, and δ components of the Mo–Mo quadruple bond.

Experimental Section

$Mo_2(O_2CCH_3)_4$ was prepared by literature techniques[22] and purified by sublimation on a Schlenk line. Thin films ($\approx$100 Å or less) of $Mo_2(O_2CCH_3)_4$ were vapor deposited in ultrahigh vacuum on graphite and MoS_2 substrates, and the He I spectra (Vacuum Generators ESCALAB Mk II) were compared to previously reported spectra.[12] The previous results were reproduced. The $Mo_2(O_2CCH_3)_4$ was then sealed in ampules under vacuum for transport to the synchrotron source.

High-resolution photoemission experiments were conducted with the Minnesota Argonne extended-range grasshopper beam line at the Wisconsin Synchrotron Radiation Center. In this case, thin films of $Mo_2(O_2CCH_3)_4$ were deposited on mirror-like n-type GaAs(110) surfaces that had been prepared by cleaving in situ. The film thicknesses were determined with a quartz-crystal thickness monitor. The operating

(5) (a) Casas, J. M.; Cayton, R. H.; Chisholm, M. H. *Inorg. Chem.* **1991**, *30*, 358. (b) Cotton, F. A.; Faucilo, L. R.; Reid, A. H.; Roth, W. J., Jr. *Acta Crystallogr., Sect. C:Cryst. Struct. Commun.* **1990**, *C46(10)*, 1815. (c) Kerby, M. C.; Eichhorn, B. W.; Doviken, Lu; Volkhart, P. C. *Inorg. Chem.* **1991**, *30(2)*, 156. (d) Cotton, F. A.; Wiesinger, K. J. *Inorg. Chem.* **1990**, *29(14)*, 2594.

(6) (a) McCarley, R. E.; Carlin, R. T. *Inorg. Chem.* **1989**, *28*, 3432. (b) McCarley, R. E.; Ryan, T. R. *Inorg. Chem.* **1982**, *21*, 2072.

(7) (a) Cayton, R. H.; Chisholm, M. H.; Huffman, J. C.; Lobkovsky, E. B. *Angew. Chem., Int. Ed. Engl.* **1990**, *12*, 1481. (b) Cayton, R. H.; Chisholm, M. H. *J. Am. Chem. Soc.* **1989**, *111*, 8921. (c) Cayton, R. H.; Chisholm, M. H.; Huffman, J. C., Lobkovsky, E. B. *J. Am. Chem. Soc.* **1991**, *113*, 8709.

(8) (a) Kerby, M. C.; Eichhorn, B. W. U.S. Patent 4965381; *Chem. Abstr.* **1991**, *114*, 151429. (b) Kerby, M. C.; Eichhorn, B. W. U.S. Patent 4916222; *Chem. Abstr.* **1990**, *113*, 90360.

(9) Cotton, F. A. *Acc. Chem. Res.* **1978**, *11*, 225 and references therein.

(10) Green, J. C.; Hayes, A. J. *Chem. Phys. Lett.* **1975**, *31(2)*, 306.

(11) Lichtenberger, D. L.; Blevins, C. H. *J. Am. Chem. Soc.* **1984**, *106*, 1636.

(12) Lichtenberger, D. L.; Kristofzski, J. G. *J. Am. Chem. Soc.* **1987**, *109*, 3458.

(13) Kristofzski, J. G. *Diss. Abstr. Int. B* **1988**, *49(5)*, 1691.

(14) Brennan, J. G.; Green, J. C.; Redfarn, C. M. *J. Am. Chem. Soc.* **1989**, *111(7)*, 2373.

(15) Cooper, G.; Green, J. C.; Payne, M. P.; Dobson, B. R.; Hillier, I. H. *J. Am. Chem. Soc.* **1987**, *109*, 3836.

(16) Brennan, J. G.; Green, J. C.; Redfern, C. M.; MacDonald, M. A. *J. Chem. Soc., Dalton Trans.* **1990**, 1907.

(17) Cooper, G.; Green, J. C.; Payne, M. P. *Mol. Phys.* **1988**, *63(6)*, 1031.

(18) Butcher, K. D.; Didziulis, S. V.; Briat, B.; Solomon, E. I. *J. Am. Chem. Soc.* **1990**, *112*, 2231.

(19) Didziulis, S. V.; Cohen, S. L.; Gerwith, A. A.; Solomon, E. I. *J. Am. Chem. Soc.* **1988**, *110*, 250.

(20) Didziulis, S. V.; Cohen, S. L.; Butcher, K. D.; Solomon, E. I. *Inorg. Chem.* **1988**, *27*, 2238.

(21) Yeh, J. J.; Lindau, I. *At. Data Nucl. Data Tables* **1985**, *32*, 1.

(22) Cotton, F. A.; Mester, Z. C.; Webb, T. R. *Acta Cryst. B.* **1974**, *30*, 2768.

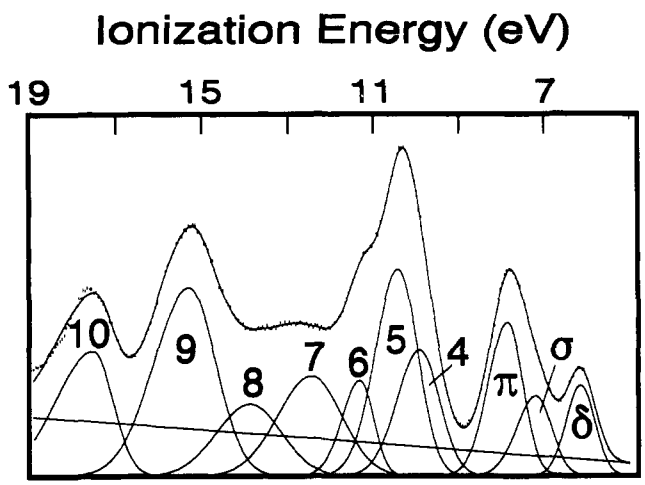

Figure 2. Valence region photoelectron spectrum at 50-eV source energy. The small dashes are the experimental data. The solid line is the sum of the numbered peaks and base line.

pressure was $<2 \times 10^{-10}$ Torr during the experiments. The synchrotron radiation beam was incident at 45° with respect to the surface normal. Photoelectrons were collected with an angle-integrated double-pass cylindrical mirror analyzer with its axis at 45° to the substrate surface normal. The overall instrument resolution (photons plus electrons) was typically 0.3 eV for photons in the energy range 40–90 eV. Higher resolution spectra (0.13–0.2 eV) were also acquired and they showed the feature labeled as the σ ionization in Figure 1 more clearly, confirming the 21.2 eV spectrum of ref 12.

The relative areas (cross sections) of the valence ionization bands were determined using program GFIT.[23] This program models the valence ionization bands with asymmetric Gaussian peaks by methods and criteria as described elsewhere.[23,24] The spectrum collected with the 50-eV source energy was the first spectrum to be analyzed in detail. This spectrum was chosen first for two reasons. First, the resolution and relative intensities of the ionizations allow the best overall identification of individual peaks and, second, the source energy is an intermediate value in the range of source energies that are used. The individual peaks are defined by their position, amplitude, a half-width for the high binding energy side of the peak, and a half-width for the low binding energy side of the peak. A minimum number of peaks and parameters are used to model the visible contours of the bands. When two peaks are significantly overlapping, it should be remembered that the individual parameters are not independent, and physical significance should only be given to the overall fit. The positions were the same in all of the spectra within experimental error (±0.02 eV). In the analysis of subsequent spectra, the peak half-widths and intensities were allowed to vary to compensate for differences in resolution and cross section brought about by changing the source energy. The peak widths were reproducible to ±0.02 eV ($\sim 3\sigma$) for each spectrum. The uncertainty in the absolute areas is about 10% with the primary uncertainty arising from definition of the base line. However, the reproducibility of the areas for purposes of comparison is within a few percent because the base line is chosen consistently.

For comparison of the cross sections between the spectra, the intensities were normalized according to the incident photon intensity during data collection. An alternative approach is to choose an ionization in the spectrum as a standard, and then compare all other cross-section changes to the cross section for this ionization. This approach led to the same conclusions for the character of the ionizations, but is more difficult to present clearly and will not be discussed. The alternative approach to analysis did serve as a check that the measurement of the incident photon intensity was consistent and did not introduce any artifacts to the interpretation.

Results

The valence region photoelectron spectrum of $Mo_2(O_2CCH_3)_4$ that was obtained with a source energy of 50 eV is shown in Figure 2. The relative positions of the ionizations agree with previous results from gas-phase[11] and thin film[12] ($Mo_2(O_2CCH_3)_4$ on gold) photoelectron spectra. The ionization energy scale in Figure 2 is adjusted so that the position of peak 1 matches the position of this peak referenced to the vacuum level in the gas-phase photoelectron spectrum. The spectrum is modeled analytically with 10 asymmetric Gaussian peaks. This is a minimum number of peaks to account for the observable band contours and the changes in intensity that occur in different regions of the spectrum with changes in photon energy. These peaks provide an adequate analytical representation of the data, but should not be interpreted in terms of individual ion states except as noted in the Discussion. The inclusion of more peaks in the analytical model would improve the total fit, particularly in the region of peak 10, but is not justified for the purposes of the present study.

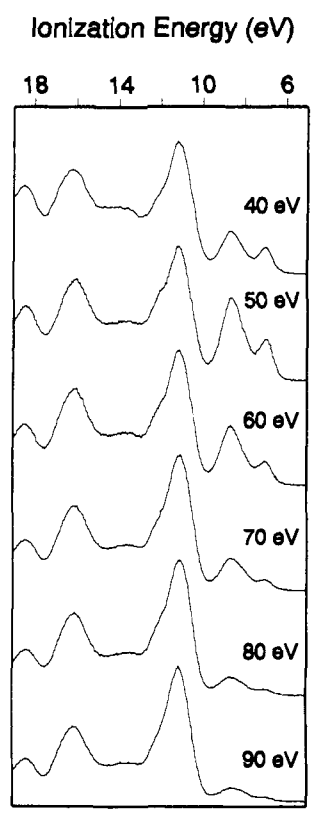

Figure 3. Valence region photoelectron spectra collected with source energies 40–90 eV.

The sample of $Mo_2(O_2CCH_3)_4$ on GaAs was prepared sufficiently thick so that the ionizations of the GaAs substrate are not visible for this range of source energies, but not so thick that charging and broadening effects significantly degrade the data. The extent of broadening from solid-state effects is evident from comparing the 0.80-eV width of the first ionization band in this spectrum with the 0.34-eV width of the vibrational envelope of the first ionization band of $Mo_2(O_2CCH_3)_4$, which is known from the high-resolution gas-phase photoelectron studies of this molecule.[11] The total photon source and electron kinetic energy analyzer resolution of the synchrotron studies is 0.3 eV compared with 0.02 eV resolution for the HeI studies of the gas-phase species.

The valence region photoelectron spectra collected at a variety of incident photon energies are presented in Figure 3 and Figure 4. Figure 3 shows the spectra collected in 10-eV increments of source energy between 40 and 90 eV, and Figure 4 shows the spectra collected at 40-, 43-, 45-, 47-, and 50-eV source energy. These plots give a visual picture of the most important relative changes in cross sections with source energy. It can be seen that the cross sections of the first three peaks (labeled δ, σ, and π) in Figure 2 remain strong in the range 40–60 eV, in comparison with the remainder of the spectrum. These cross sections fall off dramatically at higher source energies. These peaks are associated with the primary metal character, and the detailed analysis of these cross sections provides specific information on the nature of the quadruple metal–metal bond.

The areas obtained from the fits of the spectra are normalized (as described in the Experimental Section) for comparisons be-

(23) Lichtenberger, D. L.; Fenske, R. F. *J. Am. Chem. Soc.* **1976**, *98*, 50.
(24) Lichtenberger, D. L.; Copenhaver, A. S. *J. Electron Spectrosc. Relat. Phenom.* **1990**, *50*, 335.

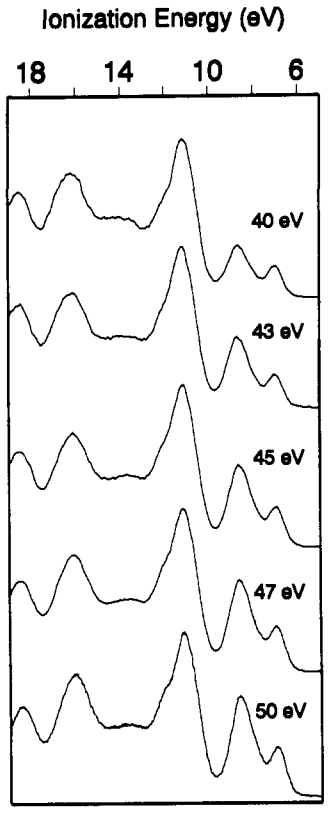

Figure 4. Valence region photoelectron spectra collected with source energies 40–50 eV.

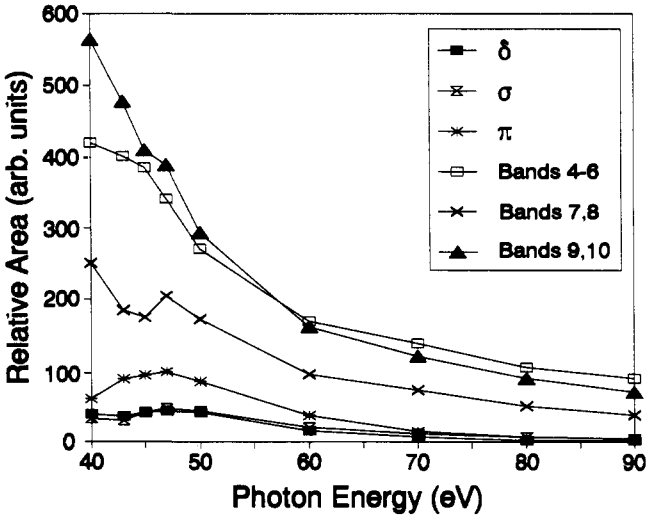

Figure 5. Relative cross sections for all peaks in the valence region.

tween the spectra collected at different source energies. Figure 5 shows the results of these comparisons by plotting the cross section for each peak (or group of peaks) against the incident photon energy. For the most part, the cross sections of peaks 4–6 and 9–10 drop off with increasing source energy. This behavior is predicted for ionization of orbitals which have a large amount of carbon and oxygen character.[21] A noticeable aberration to this occurs at around 47 eV, where the cross sections for peaks 4–6 and 9–10 do not decrease uniformly. The other peaks actually show an increase in total cross section in this region of source energy.

Figure 6 shows the effect of changing the incident photon energy on the cross section of the first three ionizations. The cross sections for these ionizations show a maximum centered at 47 eV. Peaks 7 and 8 also go through a maximum in the region of 47 eV. After the maximum at 47 eV, the cross sections of the peaks labeled δ, σ, and π decrease uniformly and more dramatically than peaks

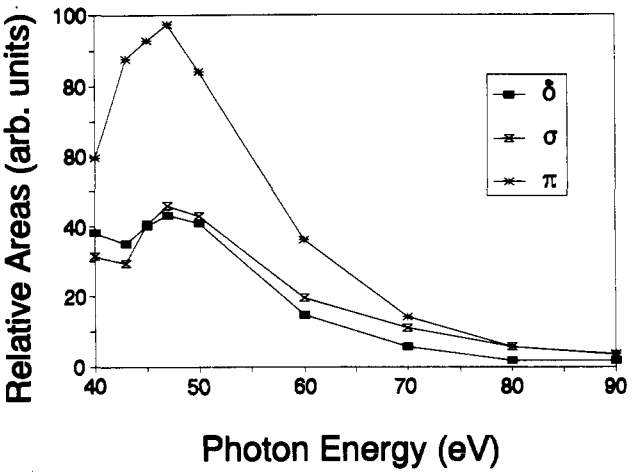

Figure 6. Relative cross sections for ionizations of the Mo–Mo bond.

4–6 and 9–10. These observations are particularly significant to the interpretation of the ionizations.

Discussion

General assignments of the ionizations arising from the metal–metal bonds and the ligand-based orbitals of $Mo_2(O_2CCH_3)_4$ have been provided by previous photoelectron[3,10,12] and computational studies.[2,25] The leading ionization at 6.98 eV (referenced to the vacuum level in the corresponding gas-phase spectrum) is assigned to the Mo–Mo δ bond (and is labeled as such in Figure 2). The Mo–Mo σ and π ionizations are also labeled as such in Figure 2. The Mo–Mo σ bond ionization is not observed as a completely separate band, as is discussed in more detail below. The peaks labeled 4–6 arise from oxygen lone pairs and Mo–O interactions. Peaks 7–8 result primarily from the ionization of Mo–O σ bonds and C–O π bonds, and peaks 9–10 include C–C and other ligand σ bonding interactions. Because of the large number of ion states in the region of peaks 4–10 and the degrees of freedom in the fit (in reality many more peaks are overlapping in this region), peaks 4–10 in the spectra will not be discussed in detail. However, they are included for a general comparison of the changes in cross sections.

Although the metal–metal δ and π ionizations were easily identified in the initial photoelectron studies of quadruple-bonded dimolybdenum complexes, direct observation and characterization of the metal–metal σ ionization has been much more difficult. In the high resolution gas-phase photoelectron spectroscopy studies of dimolybdenum complexes, no ionization has been observed that can be assigned to the metal–metal σ ionization. It is now apparent that the Mo–Mo σ and π ionizations are coincident in the gas-phase photoelectron spectrum. In the thin film spectrum shown in Figure 2, an asymmetry is observed on the low ionization side of the π band that is assigned to the σ ionization. The total band envelope in this region is better fit with two peaks, one at 8.02 eV (labeled σ in the spectrum) and another at 8.71 eV (labeled π in the spectrum), which have approximate relative areas of 1:2. A similar broadening and asymmetry is not observed on the δ ionization, thus ruling out external sample or instrumentation effects. The ionization intensity on the low ionization energy side of the π band is also observed in the He I surface spectra of $Mo_2(O_2CCH_3)_4$ on gold, MoS_2, and graphite substrates,[12] thus also ruling out effects of the substrate. The peak on the low ionization energy side at 8.02 eV is assigned to the Mo–Mo σ bond, and the larger peak at 8.71 eV is assigned to the Mo–Mo π bond.

In our previous surface photoelectron spectra of thin films of $Mo_2(O_2CCH_3)_4$ on gold, the broadening and asymmetry on the low binding energy side of the π ionization band was predicted based on the assumption that the σ and π ionizations are coincident in the gas phase, and on the expectation that the σ ionization is

(25) (a) Ziegler, T. *J. Am. Chem. Soc.* **1985**, *107*, 4453. (b) Ziegler, T.; Tschinke, V.; Becke, A. *Polyhedron* **1987**, *6*, 685.

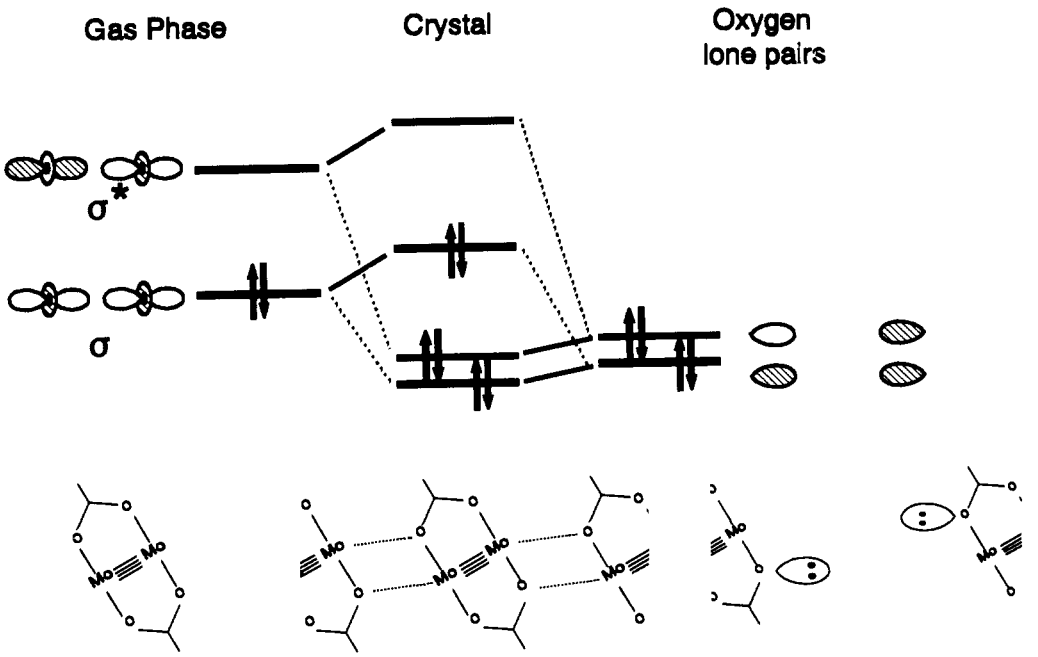

Figure 7. Qualitative molecular orbital scheme showing intermolecular interactions in bulk samples of $Mo_2(O_2CCH_3)_4$.

shifted to lower ionization energy relative to the π in the solid state.[12] Figure 7 shows the origin of the electronic perturbation in the solid state that shifts the σ ionization to lower energy. The axial position of the Mo–Mo bond is a weak coordination site, and the $Mo_2(O_2CCH_3)_4$ molecules tend to orient in the solid with the oxygen atom from the acetate of one molecule in the axial position of the Mo–Mo bond of another molecule, as shown on the bottom of Figure 7. The intermolecular Mo–O distance, determined by crystallographic data[22] of 2.645 Å is somewhat longer than a typical Mo–O covalent bond length of 2.20 Å, but the distance is small enough to significantly perturb the Mo–Mo σ bond. Figure 7 shows how the lone pairs of electrons on the oxygen atoms interact with the Mo $4d_{z^2}$ orbitals on the adjacent molecule to destabilize the σ ionization. The other consequence of this interaction is the stabilization of the oxygen lone pair ionizations. This effect, however, is not observable owing to the overlapping peaks in that region (peaks 4–5 in Figure 2). The destabilization of the σ bond removes the degeneracy of the σ and π ionizations that is found in the gas phase. Other than this relative shift of the σ ionization, there are no other significant variations in the relative positions of the ionization peaks from the gas-phase to the thin film spectra.

The changes in photoionization cross sections with source energy are consistent with these assignments. The cross sections for peaks 4–6 and 9–10 decrease fairly steadily with increasing source energy, as expected for their primary ligand character. The most significant variation in photoionization cross section with source energy is the enhanced intensity of some of the valence ionization bands near a source energy of 47 eV. This corresponds to a p $\rightarrow$ d giant resonant enhancement that is characteristic of d-block transition metal compounds. This enhancement autoionizes through a super-Coster–Kronig (SCK) Auger decay process[26] and occurs in addition to the direct ionization which is normally observed in this experiment. For example, in the case of compounds containing molybdenum formally in the 2+ oxidation state ($4p^64d^4$ electron configuration), such as in $Mo_2(O_2CCH_3)_4$, the ionization processes are:

$$4p^64d^4 \xrightarrow{h\nu} 4p^64d^3 + e^- \quad \text{direct ionization}$$

$$4p^64d^4 \xrightarrow{h\nu} 4p^54d^5 \rightarrow 4p^64d^3 + e^- \quad \text{enhancement ionization}$$

The direct ionization simply involves ejection of a valence 4d electron by the incident photon. The enhancement channel for ionization is thought of in terms of two components. The first component involves the resonant excitation of one of the 4p electrons into a 4d orbital by the photon. The second component involves relaxation of a 4d electron from the excited state back to the 4p shell with simultaneous ejection of a 4d electron in an Auger-type decay process. It should be noted that the starting and ending configurations of these two processes are identical. They are indistinguishable in terms of the energy absorbed and the kinetic energy of the leaving electron, yet they are two distinct channels for ionization. As a consequence, when the incident photon energy is of the correct frequency, both processes occur and the cross section for ionization from the Mo 4d orbitals is resonant enhanced.

This resonant enhancement occurs for other metal complexes at an energy nearly equal to the ionization energy of the transition metal np (where n is the valence shell) electrons. In some systems this phenomenon creates a "double hump" enhancement in the cross-section profiles because of the small difference in energy between the spin–orbit split metal $np_{1/2}$ and $np_{3/2}$ ionizations. For reference, the calculated values for the Mo ionizations are 42 and 45 eV,[21] which compare well to the experimental enhancement values reported for $Mo(CO)_6$ of 42 and 46.5 eV.[15] The "double hump" observed in the variable-energy PES experiments performed on $Mo(CO)_6$ is not observed in this study of $Mo_2(O_2CCH_3)_4$. The absence of the double hump in this study of $Mo_2(O_2CCH_3)_4$ might be attributed to several sources. It is possible that, because the spectra were collected at only every 2–3 eV in source energy, this "double-hump" was missed because of an insufficient density of data points. However, the appearance of the curves in Figure 3 and Figure 4 does not suggest that this is the case. Alternatively, $Mo_2(O_2CCH_3)_4$ has a lower symmetry and many more electronic states than $Mo(CO)_6$, and the second smaller enhancement may be masked owing to broadening from overlap with the ligand based orbitals. In addition, the overlap of the metal 4d orbitals with the neighboring metal 4d and even 4p orbitals in these metal dimers may also be an important factor that spreads the energy of the ion states and broadens the maximum. This point is discussed in more detail later.

The extent that an ionization cross section is enhanced by the resonance process is related to the amount of Mo 4d character associated with the ionization. This enhancement is most pronounced for the ionization assigned to the Mo–Mo π bond. The enhancement in the σ and δ ionizations is smaller, thus indicating that the Mo 4d contribution to the σ and δ components is less than

(26) (a) Davis, L. C. *Phys. Rev. B: Condens. Matter* **1982**, *25*, 2912. (b) Davis, L. C.; Feldkamp, L. A. *Phys. Rev. B: Condens. Matter* **1981**, *23*, 6239.

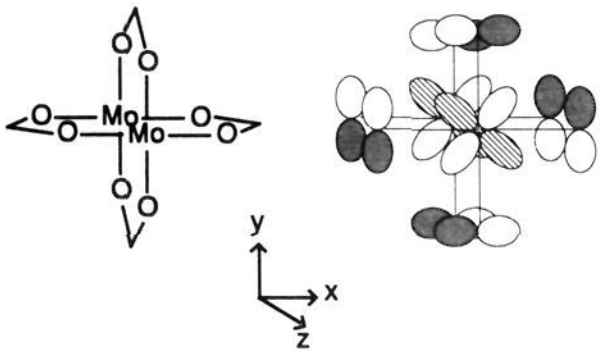

Figure 8. Interaction of the Mo–Mo δ bond (composed of d_{xy} orbitals) with the oxygen p orbitals.

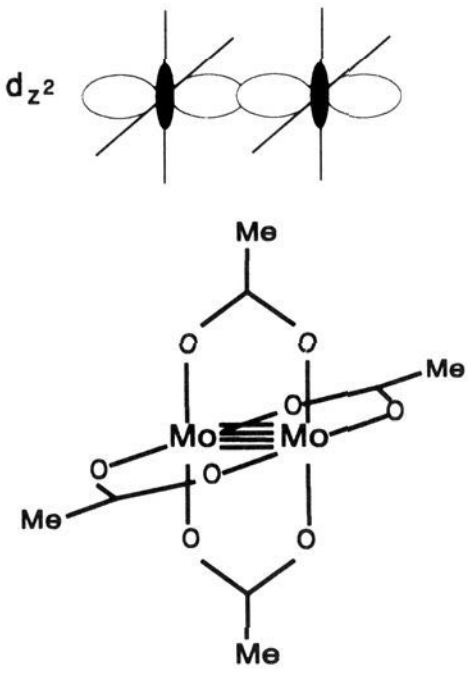

Figure 9. Diagram showing the interaction of the σ bond with the oxygen atoms on the carboxylate ligands. The shaded portion of the d_{z^2} orbital is oriented to interact with the oxygens.

that for the π components. This experimental result agrees with previous suggestions about the nature of the components in the Mo–Mo quadruple bond.[2,25]

In the case of the δ bond, the Mo d_{xy} orbitals on the two metals (Figure 1) interact not only with each other, but also with the oxygen p orbitals that are perpendicular to the plane of the carboxylate ligand. The symmetry of the metal–oxygen interaction in the δ ionization is shown in Figure 8. The carboxylate orbital is the symmetric p_π combination. This filled–filled interaction gives the δ bond some ligand character, which in turn lessens the observed enhancement in the cross section of this band in the variable-energy PES experiment. The filled symmetric p_π combinations of the carboxylate ligands ionize in the region of bands 4–6 in the spectrum. The cross sections for the ionizations in this region decrease smoothly with increasing source energy, except for a small aberration in the region of 47 eV. This is consistent with a small amount of metal character in these ionizations. By symmetry, the mixing of the orbitals in this region with the metal must be with the δ orbital.

The Mo–Mo σ ionization may gain some ligand character by the interaction shown in Figure 9.[2] The d_{z^2} orbital has the correct symmetry to interact with the oxygen atoms in a σ fashion. This filled–filled interaction will diminish the magnitude of this enhancement of the σ ionization near 47 eV. Interestingly, the ionizations in the region of peaks 7 and 8 also show a maximum in their cross sections around 47 eV. This region has been assigned to include the Mo–O σ bonds, and the cross-section behavior indicates some metal character with these ionizations.

The metal–metal σ ionization may also have a contribution from the Mo $4p_z$ orbitals,[2] which will also dampen the enhancement. As shown in Figure 10, the $4d_{z^2}$ orbital in the σ bond has the correct symmetry to interact with the $4p_z$ orbital on the adjoining metal atom. This interaction will also split the 4p levels. As mentioned earlier, the splitting of the 4p levels may also explain the broad maximum in cross section that we see at 47 eV in

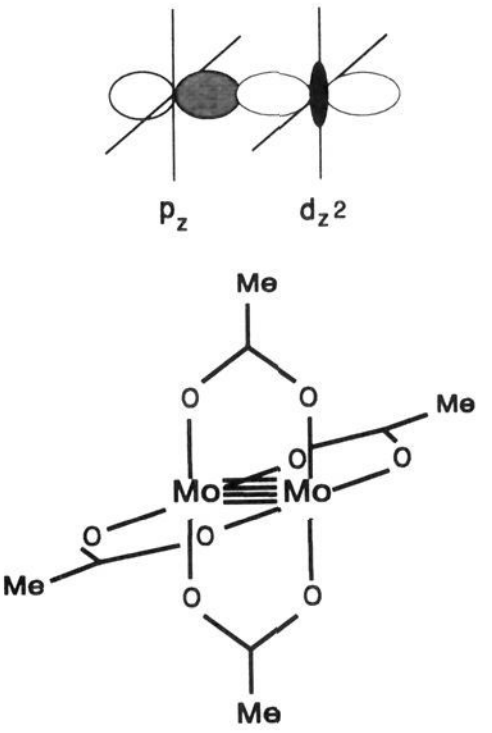

Figure 10. Interaction of a Mo d_{z^2} orbital with the p_z orbital on the adjoining Mo.

contrast to the "double hump" maximum that has been observed in the spectra of mononuclear complexes. The role of the 4p orbitals in the valence σ ionization is a topic of continuing investigation.

Turning back now to the ionization from the Mo–Mo π bonds, it is seen that these orbitals do not have as much mixing with the carboxylate ligands as their σ and δ counterparts. The metal–metal π bonds are formed from the d_{xz} and d_{yz} orbitals (Figure 1), which do not have the correct symmetry to interact with the carboxylate π orbitals and which do not have as much overlap with the oxygen lone pairs. Thus the Mo–Mo π ionizations retain the most Mo 4d character and show the largest resonant enhancement.

The observations of changes in ionization cross sections with excitation energy show the effects of the interactions, but do not readily lend themselves to giving an accurate quantitative measure of the amount of Mo 4d character in the valence orbitals in this case. Part of the difficulty is the overlap of several valence ionizations which increases the uncertainty in the determination of their areas. More research is needed to gain a more precise understanding of the Mo 4d contributions to these levels. Nonetheless, a rough estimate may be obtained by looking at the cross section of each ionization at the pre-enhancement minimum (which occurs in the region of 40–43-eV source energy) in comparison to the cross section at the enhancement maximum (which occurs near 47-eV source energy). The cross section for the π ionization increases 66% from the pre-enhancement minimum to the maximum, the σ ionization increases 55%, the δ ionization increases 24%, and peaks 7 and 8, which include the Mo–O σ bonds, increase 17%. The trends reflected by these numbers support previous proposals[2] concerning the nature of the metal–metal quadruple bond. Specifically, the π components are the greatest contributors to the overall metal–metal bond strength. The valence σ and δ components, partly because of their overlap with ligand orbitals, have less of a contribution to the overall metal–metal bond strength.

Acknowledgment. D.L.L. and C.D.R. acknowledge the National Science Foundation (Grant CHE8519560) for support of this work. D.L.L. acknowledges support by the U.S. Department of Energy (Division of Chemical Sciences, Office of Basic Energy Sciences, Office of Energy Research, DF-SG02-86ER13501) for contributions to the equipment, and the Materials Characterization Program, Department of Chemistry, University of Arizona. J. H.W., F.S., and Y.C. were supported by the National Science Foundation (DMR 91-08419). The photoemission experiments were done at the Wisconsin Synchrotron Radiation Center, a user facility supported by the NSF, and the assistance by the staff of the laboratory is gratefully acknowledged.